International Journal of Nanomedicine Dovepress

Open Access Full Text Article ORIGINAL RESEARCH

Nasal mRNA Nanovaccine with Key Activators of Dendritic and MAIT Cells for Effective Against Lung Tumor Metastasis in Mice Model

Ang Li[1,*], Xushan Cai[2,*], Dong Li[1,*], Yimin Yu[1], Chengyu Liu[1], Jie Shen[1], Jiaqi You[3], Jianou Qiao[3], Feng Wang[4]

[1]Department of Laboratory Medicine, Shanghai Tongji Hospital, School of Medicine, School of Life Science and Technology, Tongji University, Shanghai, People's Republic of China; [2]Department of Clinical Laboratory, Shanghai Jiading Maternal and Child Health Hospital, Shanghai, People's Republic of China; [3]Department of Respiratory, Shanghai Ninth People's Hospital Affiliated Shanghai JiaoTong University School of Medicine, Shanghai, People's Republic of China; [4]Department of Thoracic Surgery, Shanghai Ninth People's Hospital Affiliated Shanghai Jiao Tong University School of Medicine, Shanghai, People's Republic of China

*These authors contributed equally to this work

Correspondence: Ang Li, Department of Laboratory Medicine, Shanghai Tongji Hospital, School of Medicine, School of Life Science and Technology, Tongji University, No. 389 Xincun Road, Shanghai, 200065, People's Republic of China, Email liang@tongji.edu.cn; Feng Wang, Department of Thoracic Surgery, Shanghai Ninth People's Hospital Affiliated Shanghai Jiao Tong University School of Medicine, No. 639, Zhizaoju Road, Shanghai, 200011, People's Republic of China, Email wangsongyi1997@163.com

Background: Lung metastasis is a leading cause of cancer-related death. mRNA-based cancer vaccines have been demonstrated to be effective at inhibiting tumor growth. Intranasal immunization has emerged as a more effective method of inducing local immune responses against cancer cells in the lungs.

Methods: An innovative layered double hydroxide- and 5-OP-RU–based mRNA nanovaccine (Mg/Al LDH-5-OP-RU/mRNA) was synthesized via coprecipitation. The particle size distribution and zeta potential were measured, and the nanovaccine was observed by transmission electron microscopy. The functions and properties of the nanovaccine were evaluated via an mRNA-targeted delivery assay and measurement of dendritic cell (DC) and mucosa-associated invariant T (MAIT) cell maturation and activation. In addition, the cytotoxicity, antigen-specific T cell activation, cytokines, protective ability, and therapeutic ability of the nanovaccine were assessed in a mouse tumor model. Further, the immune cell composition was evaluated in tumors.

Results: The Mg/Al LDH-5-OP-RU/mRNA nanovaccine was efficiently delivered into lung-draining mediastinal lymph nodes (MLNs), and it activated dendritic cells (DCs) and mucosa-associated invariant T (MAIT) cells after intranasal administration. Moreover, the optimized dual-activating mRNA nanovaccine efficiently transfected DC cells and expressed antigen proteins in DC cells. An HPV-associated tumor model revealed that the intranasal delivery of the Mg/Al LDH-5-OP-RU/E7 mRNA nanovaccine significantly prevented the lung metastasis of tumors and had a therapeutic effect on established metastatic tumor nodules in the lungs. Mechanistically, the enhanced activation of DC and MAIT cells induced by the Mg/Al LDH-5-OP-RU/E7 mRNA nanovaccine increased the production of immune-stimulating cytokines and decreased the secretion of immunosuppressive cytokines, which led to the expansion and activation of memory T cells targeting the E7 antigen, a reduction in the population of neutrophils, and differentiation of tumor -associated macrophages to the M1 phenotype in the lungs.

Conclusion: These results highlight the potential of the innovative nasal mRNA nanovaccine for both preventing and treating tumor metastasis in the lungs.

Keywords: mRNA nanovaccine, layered double hydroxide, 5-OP-RU, dendritic cells, Mucosa-associated invariant T cells, lung metastasis

Introduction

The majority of cancer-related fatalities are caused by the spread of cancer cells to distant parts of the body rather than the initial tumor. The incidence of lung metastasis in cancer patients ranges from 20% to 54%, making it a major

Received: 24 May 2024
Accepted: 29 October 2024
Published: 8 November 2024

contributor to morbidity and mortality in individuals with advanced cancer.[1] A viable strategy to inhibit lung metastasis may be to induce antitumor immunity against cancer cells that have migrated to the lungs. Intranasal immunization has emerged as a more effective method of inducing local immune responses in the lungs and activating pulmonary tissue-resident memory T cells, which can provide protection against tumor challenges.[2,3] On the basis of these traits, there is strong interest in developing nasal vaccines that can effectively stimulate local immune responses in the lungs to combat lung metastatic cancer.

Given the remarkable efficacy demonstrated by mRNA vaccines in combating SARS-CoV-2, it is highly probable that mRNA-based therapies will also play a significant role in the development of cancer vaccines.[4,5] The use of nanobiotechnology tools to create antigen-loaded particles with optimal encapsulation and targeting capabilities is crucial for enhancing the effectiveness of mRNA vaccines in enhancing mucosal immune responses. Currently, there are numerous delivery systems for mRNA vaccines that utilize nanoparticles to induce T cell responses in mouse models of infection and cancer.[6] These systems have been extensively researched and developed with a focus on material properties.[7–9] However, the immune routes of mRNA tumor vaccines are mainly through subcutaneous injection, intramuscular injection, and intravenous injection. These injection routes often limit the transportation of nanovaccines. Compared with traditional immunization methods, intranasal immunization can allow vaccines to accumulate in alveolar and bronchial associated lymphoid tissues, making it easier to promote the activation and uptake of lung lymphocytes, induce stronger tissue resident T cell immunity in the lungs,[10,11] and have significant advantages in the application of immunotherapy for lung tumors. So far, a few studies have examined the efficacy of NP-based nasal vaccines in specifically activating lung-resident CD8+ T cells against cancer cells.[12,13] This underscores the importance of developing, improving, and analyzing NP-based nasal mRNA vaccines to boost memory T cell numbers in the pulmonary region to prevent lung metastasis of cancer cells.

We previously developed a novel inorganic nanocarrier based on the intercalation properties of layered double hydroxide (LDH). Our experiments revealed that this new nanomaterial as a vaccine carrier has several significant advantages. First, the new inorganic nanomaterial completely encapsulates biomolecules in the main layer, and the formation of neutral interlayer complexes minimizes the electrostatic repulsion between negatively charged cell membranes and biomolecules, thereby accelerating the transfer of biomolecules to cells.[14] Second, the layered inorganic material acts as a "molecular switch" and can control its release rate by adjusting the pH. In an environment with a pH of 4–5, drugs are released quickly, which is helpful for fully releasing mRNA in the endosomal environment of dendritic cells (DCs) or macrophages.[15,16] Third, LDH has an immunostimulatory effect and can stimulate DC maturation to some extent, upregulating the expression of costimulatory molecules, such as MHC-II, CD80/CD86, and CD40.[17,18] Fourth, because the degradation products are inorganic compounds, they do not cause an immune response against the material itself.[19] Finally, the conditions required for synthesizing LDH nanoparticles are relatively mild and do not cause denaturation or damage to bioactive substances. We have previously successfully used LDH as a vaccine carrier in the development of melanoma and hepatitis B DNA vaccines.[17,20,21] In vivo experiments have shown that melanoma DNA vaccines and hepatitis B DNA vaccines using LDH as a carrier significantly increase the activation of CD8+ T cells and antibody titers. The melanoma DNA vaccine using LDH as a carrier not only has good protective effects but also has a certain therapeutic effect, significantly inhibiting tumor growth in tumor-bearing mice.

Recent research has demonstrated that the activation of mucosal-associated invariant T (MAIT) cells, triggered by microbial metabolites from vitamin B2 biosynthesis (such as 5-(2-oxopropylideneamino)-6-D-ribitylaminouracil, 5-OP-RU), can enhance mucosal immune defenses and contribute to overall protection.[12–23] Studies have shown a direct link between the activation of MAIT cells and the robust T cell responses induced by vaccines in both humans and mice, which exhibit weakened vaccine induced CD8+ T cell responses to various antigens. MAIT cells play a crucial role as intermediaries between the innate and adaptive immune systems.[24]

Agonists, such as 5-(2-oxoethylideneamino)-6-D-ribitylaminouracil (5-OE-RU) and 5-OP-RU, which are naturally synthesized by the condensation of 5-amino-6-D-ribitylaminouracil (5-A-RU) with glyoxal and methylglyoxal (MG), have been identified.[25] Stimulation of MAIT cells in the lung has been demonstrated through treatment with MAIT cell agonists in combination with Toll-like receptor (TLR) agonists[26,27] or some cytokines.[28]

These study highlighted the ability of a pH-sensitive Mg/Al LDH nanoparticle/mRNA vaccine conjugate with 5-OP-RU to promote the uptake of DCs in lung tissue, resulting in the establishment of durable CD8+ tissue-resident memory T cells in the lungs that confer protection against tumor metastasis in the lungs. Mechanistically, the nanovaccine exerted its most prominent influence on targeting lung-draining MLNs and enhancing the maturation of DCs in MLNs. Furthermore, the administration of Mg/Al LDH-5-OP-RU nanoparticles was demonstrated to induce potent activation of MAIT cells in the mediastinal lymph nodes in the lungs, leading to enhanced cytotoxic activity of CD8+ T cells and significantly suppressing tumor seeding and metastasis in the lungs.

Materials and Methods

The in-vitro in-vivo Studies Using Mice Model

TC-1 cells expressing the E7 antigen and RAW264.7 cells Chinese Academy of Sciences (Shanghai, China) and were cultured in complete high-glucose DMEM at 37 °C and 5% CO_2. Six– to eight-week-old female C57BL/6J mice were obtained from Charles River Co. Ltd. and raised in the pathogen-free animal facility of Tongji University. All animal experimental protocols were performed in accordance with National Institutes of Health (NIH) ethical guidelines and were approved by Institutional Laboratory Animal Resources at Tongji University.

Synthesis of mRNA

The GFP or E7 cDNA was inserted into the mRNA transcription plasmid. T7 RNA polymerase was subsequently used to obtain E7 or GFP mRNA, which was then purified with an RNA purification kit (Thermofisher, USA). mRNAs were capped with the m7G capping kit (Thermofisher, USA) as previously described.[29] The reacted products were treated with DNase I and purified via an RNA purification kit (Thermofisher, USA). The mRNA products were analyzed through agarose gel electrophoresis and stored at −20 °C for future use.

Synthesis and Characterization of the Mg/Al LDH-5-OP-RU/mRNA Nanovaccine

The synthesis of Mg/Al LDH-5-OP-RU was performed through hydrothermal-assisted coprecipitation in a nitrogen atmosphere to prevent contamination from atmospheric CO_2. A mixture of $Mg(NO_3)_2$, $Al(NO_3)_3$, and 5-OP-RU (Sigma-Aldrich (Shanghai) Trading) the weight ratio of 5:5:1 ratio was prepared in sealed conical flasks with constant stirring under nitrogen gas. The pH of the solution was subsequently adjusted to 10.0. The resulting precipitates were filtered after adding 1 M NaOH solution drop by drop and stirring vigorously, and they were then reacted hydrothermally at 100 °C for 16 h. Mg/Al LDH-5-OP-RU nanoparticles were obtained by thorough washing with decarbonated water. The Mg/Al LDH-5-OP-RU/mRNA nanoparticles were synthesized by ultrasonic treatment of a mixture containing Mg/Al LDH-5-OP-RU and mRNA in the weight ratio of 10:1 at 500 rpm at 37 °C for 30 min. The zeta potential values were analyzed. The sample preparation method involved ultrasonic dispersion in PBS. SEM images were obtained using a scanning transmission electron microscope (JEM-2100F) at 100 kV voltage (Japan).

pH Control Release and RNase Protection Assay

For the pH-sensitive release assay, the PBS solutions at different pH values of 7.5, 6.5, 5.5, and 4.5 were prepared, and the Mg/Al LDH-5-OP-RU/mRNA nanoparticles were added to these solutions for 1 h. Then, 2.5 μL of loading buffer was added, followed by loading onto an agarose gel with EB dye for electrophoresis at 180 V for 8 minutes. For the RNase protection assay, naked mRNA or Mg/Al LDH-5-OP-RU/mRNA nanocomplexes were treated with either PBS or 20 ng/mL RNase A solution for 30 minutes at room temperature. These solutions were subsequently combined with 2.5 μL of loading buffer, which was subsequently loaded onto an agarose gel with EB dye for electrophoresis at 180 V for 8 minutes. The mRNA bands were visualized via a Molecular Imaging System.

Intranasal Administration of Mg/Al LDH mRNA in vivo

Mg/Al LDH-5-OP-RU/mRNA, Mg/Al LDH/mRNA, LNP/mRNA, and naked mRNA were delivered by intranasal administration in female C57/B6 mice treated with 20 μL of isoflurane. Each mouse received 6 mg of vaccine dissolved

in 50 μL of PBS. Vaccine formulations were delivered via pipet through the nostrils into the lungs of mice; All vaccines were measured to ensure that the quantity of mRNA was comparable.

Detection of Targeted Delivery of mRNA

C57BL/6J mice underwent intranasal delivery of a nanocarrier encapsulating GFP mRNA. Two days post-administration, the mice were sacrificed, and their lung tissue and lymph nodes were harvested and rinsed with 1 mL of sterile PBS. The lungs were then cut into single lobes and placed in a Petri dish for digestion via a lung dissociation kit for 6 h. After digestion, the digested tissues were passed through a 70 μm strainer to obtain a single-cell suspension. The single-cell suspension was treated with ACK lysis buffer to lyse red blood cells, which were subsequently resuspended in PBS. Then, 100 μL of fluorophore-conjugated anti-CD11c, anti-CD11b, anti-F4/80, anti-CD4, anti-α-SMA, or anti-Ly6G antibodies (details of these antibodies in Table S1) diluted in flow cytometry staining buffer was added to the single-cell suspension and incubated at 4 °C for 1 h. Subsequently, the cells were detected via a flow cytometer (BD Biosciences), and FlowJo-v10 software was used for analysis of the data.

Detection of DCs and MAIT Cells Maturation and Activation

After preparing single lymphocytes suspensions from the lung draining MLNs of vaccinated mice, and DCs were stained with 100 μL diluted fluorophore-conjugated anti-CD45, anti-CD11c antibody, anti-MHCII antibody, anti-CD80 antibody and anti-CD86 antibody; MAIT cells were stained with 100 μL diluted fluorophore-conjugated anti-CD45, MR1–5-OP-RU tetramer and anti-CD69 (Details of these antibodies in Table S1). Subsequently, the cells were detected using a flow cytometer (BD Biosciences) and FlowJo-v10 software was used for analysis of the data.

Intracellular Cytokine Staining

In total, 2×10^6 lymphocytes from the lung parenchyma and draining MLNs were isolated and stimulated with E7 protein at 1 μg/mL for 48 h. Six hours before stimulation, brefeldin A was added to block intracellular cytokine secretion. After the cells were collected, fluorescent anti-CD3 and anti-CD8 antibodies (details of these antibodies are provided in Table S1) were added, and the mixture was incubated at 4 °C for 15 min, followed by treatment with fixation buffer for 20 min at 4 °C. The fixed cells were washed with CytoPerm Wash Buffer and incubated with APC-conjugated anti–IFN-γ (Table S1) for 20 min at room temperature. After washing twice with CytoPerm Wash Buffer, the cells were detected via a flow cytometer (BD Biosciences) and analyzed via FlowJo-10.

Tetramer Labeling and Detection of E7-Specific CD8+ T Cells

After single lymphocyte suspensions were prepared from the lung-draining MLNs or tumors of vaccinated mice, 2×10^6 cells were seeded per sample and then stimulated with E7 protein (1 μg/mL) and IL-2 (20 U/mL). Next, the cells were treated with the E7 MHC class I–restricted peptide tetramer (5 μL per sample), followed by incubation with an anti-CD8 antibody for 30 minutes. Following surface staining with anti-CD3 (1:500 dilution) to assess T cells, the cells were rinsed with PBS containing 2% FBS (staining buffer) and examined using flow cytometry. FlowJo 10 software (FlowJo LLC) was utilized for data analysis after excluding doublets based on forward scatter and side scatter parameters.

Cytotoxicity Assay

Seven days after the final immunization, lymphocytes from the lung parenchyma and draining MLNs were harvested and restimulated with E7 protein (1 μg/mL) and IL-2 (20 U/mL) for 72 h. The stimulated lymphocytes were collected (effector cells) and stained with PI (20 mg/mL PI in PBS) for 20 min at 4 °C. TC-1 cells (target cells) were stained with CFSE (200 nM in 1 mL of PBS) at 37 °C for 15 min. Then, the PI-labeled effector cells were cocultured with a constant number of CFSE-labeled TC-1 cells (2×10^4) at different E(effector cells):T(target cells) ratios of (1:1, 10:1, 20:1, and 40:1) in 96-well microplates for 4 h. The resulting cell mixtures were then washed, fixed with 1% paraformaldehyde for 20 min, and analyzed via a flow cytometer (BD Biosciences). The PI-CFSE- cells represent lysed TC-1 cells, and the PI-CFSE+ cells represent living cells. The specific lysis rate for a given E:T ratio was calculated using the following equation: lysis rate = 100×(%sample lysis -% basal lysis)/100-%basal lysis.

Tumor Challenge and Bioluminescence Imaging

C57BL/6J mice were intravenously injected with 2×10^5 TC-1-luc+ cells, and 100 μL of D-luciferin was injected intraperitoneally into tumor-bearing mice to observe tumor metastasis in the lungs. The fluorescence images and intensities were detected on Days 7, 9, and 11 after tumor injection via an IVIS LUMINA III imaging system (PerkinElmer, Waltham, MA, USA). At the end of the experiment, the mice were sacrificed, and the lungs were harvested, followed by manual counting of the tumor nodes in the lungs.

Detection of Tumor Immune Cell Composition

Samples of lung tissue obtained from various study groups were fixed with 4% methanol and carefully placed onto glass slides. The tissues were permeabilized with 0.2% Triton X-100 and then blocked with 2.5% bovine serum albumin in PBS for 1 hour. The tissues were then incubated with fluorescent anti-CD11b, Ly6G, F4/80, CD206, and iNOS antibodies (antibody details are provided in Table S1) at 1:250 dilution for 1 hour. Hoechst 33342 was used to stain nuclei, and the tissues were observed under a fluorescence microscope (Leica).

BALF Collection and Cytokine Analysis

Following humane euthanasia, a solution of 100 μM EDTA and 1% protease inhibitor in PBS (1 mL) was administered into the trachea of the mice, followed by gentle aspiration. The sample was collected and transferred to a 15 mL conical tube and stored on ice. The expression of specific cytokines in the serum or BALF was analyzed via ELISA according to the manufacturer's instructions.

Biosafety Evaluation in vitro and in vivo

For biosafety evaluation in vitro, the 293T cells and DC cells were seeded in a 96-well plate at a density of 5×10^4 in each well. Followed by treatment with Mg/Al LDHs-5-OP-RU at different concentrations. After 24 h, 10 μL of CCK8 was added into the medium and kept for another 1.5 h. The optical density (OD) was measured at 450 nm by a micro plate reader. Cell viability rate was calculated as: (experimental group OD value - Blank control group OD value)/(Control group OD value - Blank control group OD value) × 100%

For biosafety evaluation in vivo, the immunized mice were euthanized and the blood samples were collected, and were sent to Center for Drug Safety Evaluation and Research, Shanghai University of T.C.M. and analyzed by a HITACHI 7080 Automatic Biochemical Analyzer.

To evaluate histopathological damage, major organs (heart, liver, spleen, lung, and kidney) were taken out and fixed in 4% paraformaldehyde overnight, then embedded in paraffin and cut into 5 mm sections for H&E staining according to standard procedures and the histology of different organs were using a light microscope (Olympus Corporation, Tokyo, Japan).

Statistical Analysis

Statistical analyses were conducted using Graph Pad 8 software. Analysis of multiple groups was performed using one-way or two way analysis of variance (ANOVA) using the Tukey post hoc test for multiple comparison within groups. The data are presented as the mean ± SD. *$p < 0.05$, **$p < 0.01$, and ***$p < 0.001$ were considered statistically significant.

Results and Discussion

Synthesis and Characterization of the Mg/Al LDH-5-OP-RU/mRNA Nanovaccine

Mg/Al LDH was conjugated with 5-OP-RU (Mg/Al LDH-5-OP-RU) through a coprecipitation technique. The Mg/Al LDH-5-OP-RU nanoparticles were subsequently combined with mRNA encoding the HPV E7 antigen at 4 °C for 30 minutes to produce Mg/Al LDH/mRNA complexes (Figure 1A). Transmission electron microscopy (TEM) images revealed that all the Mg/Al LDH-5-OP-RU/mRNA complexes had a uniform morphology of regular hexagons (Figure 1B). The particle size of the Mg/Al LDH-5-OP-RU/mRNA nanoparticle was approximately 100 nm, and the surface potential was +35 mV (Figure 1C–D). Because cell surfaces typically carry a negative charge, a higher positive

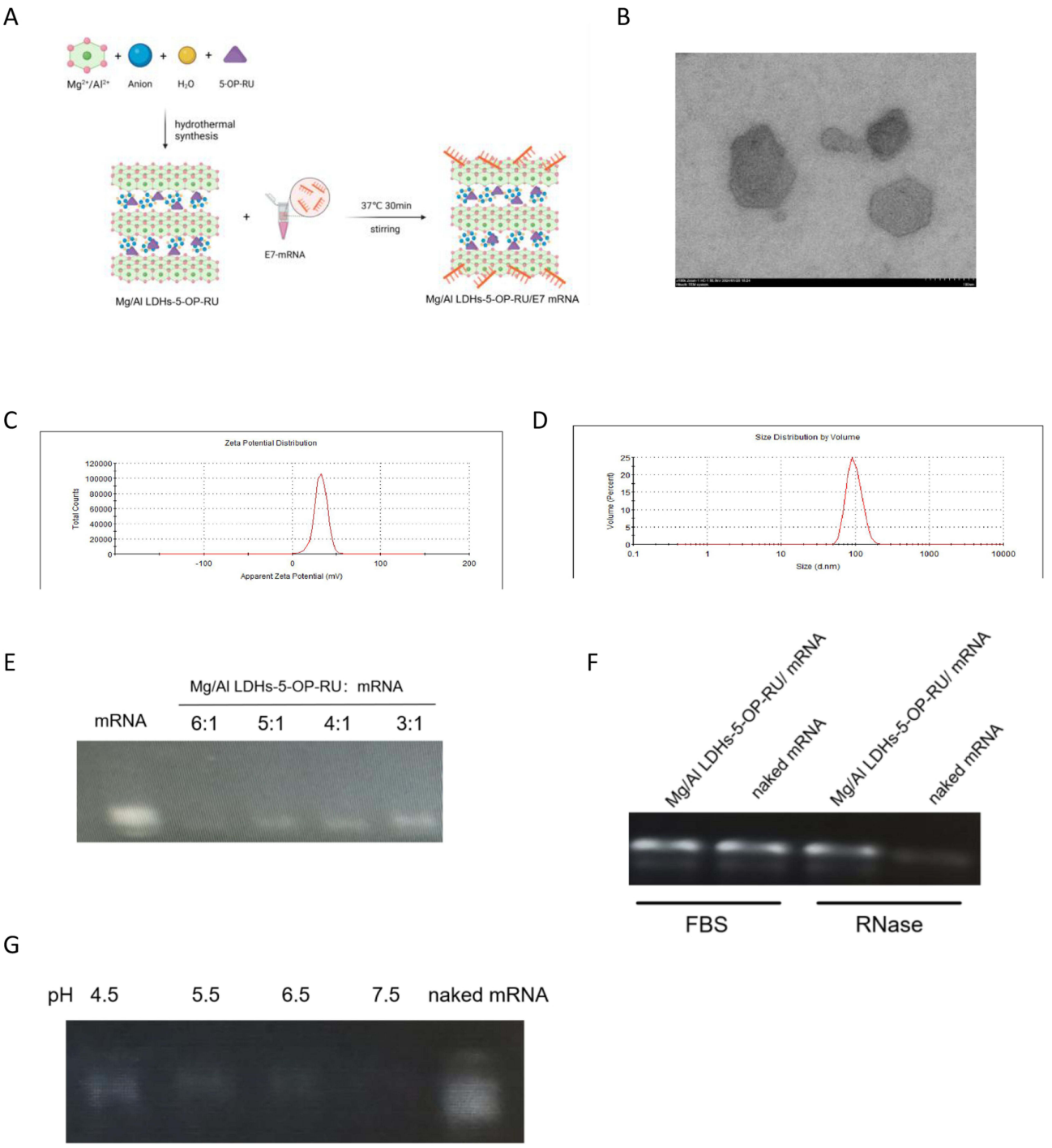

Figure 1 Synthesis and characterization of Mg/Al LDH linked with 5-OP-RU (Mg/Al LDH-5-OP-RU) for use as an mRNA delivery carrier. (**A**) Scheme illustrating the construction of Mg/Al LDH linked with 5-OP-RU. Model mRNA was encapsulated into Mg/Al LDH-5-OP-RU by the microfluidic mixing of mRNA and Mg/Al LDH-5-OP-RU. (**B**) Representative TEM image and (**C**) zeta potential of Mg/Al LDH-5-OP-RU/mRNA nanovaccines. (**D**) Size distribution of Mg/Al LDH-5-OP-RU/mRNA. (**E**) mRNA loading capacity of Mg/Al LDH-5-OP-RU at different mass ratios. (**F**) Stability of the Mg/Al LDH-5-OP-RU/mRNA nanovaccines in the present of RNase A. Samples were incubated with RNase A (10 ng/mL) at room temperature for 30 min. (**G**) Controlled release of Mg/Al LDH-5-OP-RU/mRNA by pH.

surface potential can facilitate the contact of Mg/Al LDH-5-OP-RU/mRNA with cells and increase the transfection efficiency. To observe the binding effects of Mg/Al LDH-5-OP-RU on mRNA the capacity of mRNA to bind to Mg/Al LDH-5-OP-RU was examined via the agarose gel retardation technique. As illustrated in Figure 1E, the unbound mRNA moved towards the bottom of the gel, resulting in a distinct and intense band. As the mass ratio of Mg/Al LDH-5-OP-RU

and mRNA increased, the majority of the mRNA molecules bound to Mg/Al LDH-5-OP-RU were immobilized at the top of the well, whereas the naked mRNA slowly settled at the bottom. The efficient binding of mRNA to Mg/Al LDH-5-OP-RU at a low mass ratio of 5:1 demonstrated the potential for effective mRNA vaccine delivery applications. Furthermore, to detect whether Mg/Al LDH-5-OP-RU protects mRNA vaccines from RNA enzyme degradation, Mg/Al LDH-5-OP-RU/mRNA nanovaccines were treated with RNA enzymes, and mRNA integrity was evaluated via gel electrophoresis (Figure 1F). Mg/Al LDH-5-OP-RU protected mRNAs from RNA enzyme degradation.

After antigen-presenting cells take up Mg/Al LDH-5-OP-RU/mRNA, it is crucial for mRNA to be fully released from LDH for subsequent protein translation.[30] The pH of endosomes or lysosomes in antigen-presenting cells is usually 5.5–6.5. To observe the sensitivity of Mg/Al LDH-5-OP-RU/mRNA in this pH range, Mg/Al LDH-5-OP-RU/mRNA was placed in gradient solutions with pH values ranging from 4.5 to 7.5. The Mg/Al LDH-5-OP-RU/mRNA nanovaccines were sensitive to pH, as they began to release mRNA at pH 6.5 but still effectively protected the mRNA from release at pH 7.5 (Figure 1G). These results indicated that in an in vivo physical environment with a pH of approximately 7.5, Mg/Al LDH-5-OP-RU/mRNA does not release mRNA too quickly and undergo degradation. However, once Mg/Al LDH-5-OP-RU/mRNA enters antigen-presenting cells, it can be fully released due to the lower pH of the environment inside the cells.

To evaluate the biocompatibility and biosafety of Mg/Al LDH-5-OP-RU, a CCK-8 assay was performed to detect the viability of 293T cells and bone marrow derived DCs (BMDC) after treatment with Mg/Al LDH-5-OP-RU. The results showed that Mg/Al LDH-5-OP-RU had good biocompatibility with 293T cells and BMDCs at concentrations between 10 and 320 μg mL^{-1} (Figure S1).

Delivery of Mg/Al LDH-5-OP-RU/mRNA Nanovaccine in the Lung

The lung parenchyma and draining MLNs initiate mucosal immune responses, and successful intranasal delivery of the vaccine to these sites is essential for the induction of antitumor mucosal immunity in the lung. We previously demonstrated that Mg/Al LDH efficiently accumulates in skin-draining lymph nodes after subcutaneous immunization.[18,19]

To observe the delivery efficiency of Mg/Al LDH-5-OP-RU as an mRNA vaccine carrier to the lung parenchyma and draining MLNs in vivo, fluorescent-loaded Mg/Al LDH-5-OP-RU was prepared and intranasally administered to mice. After 24 hours, the fluorescent signals were detected in the lung parenchyma of mice intranasally administered Mg/Al LDH-5-OP-RU at ~2-fold and ~1.5-fold greater levels than those of LNPs, which are widely used as mRNA vaccine carriers, and Mg/Al LDH without 5-OP-RU, respectively (Figure 2A–B, Figure S2). Furthermore, Mg/Al LDH-5-OP-RU and Mg/Al LDH were detected in the lung parenchyma and draining MLNs 72 hours after immunization, whereas LNPs almost disappeared in the parenchyma and draining MLNs 72 hours after immunization (Figure S3A–B). These results indicated that Mg/Al LDH-5-OP-RU has superior lung parenchyma and draining MLN-targeting ability, with a sustained presence in the lung parenchyma and draining MLNs.

Transfection of Mg/Al LDH-5-OP-RU/mRNA Nanovaccine in vivo

The lung parenchyma and draining MLNs provide positions where dendritic cells (DCs) stimulate specific T cell activation to generate cellular immunity that can be used in cancer immunotherapy.[31] The transfection and expression of mRNAs in DCs are crucial for initiating the specific immune response induced by mRNA vaccines. To observe whether Mg/Al LDH-5-OP-RU promotes the transfection and expression of mRNA in DCs, the mRNA encoding GFP was loaded onto Mg/Al LDH-5-OP-RU (Mg/Al LDH-5-OP-RU/GFP mRNA) and then intranasally administered to the mice. After 48 hours, the lung parenchyma and draining MLNs were collected, and single-cell suspensions were made to evaluate GFP+ DCs. As shown in Figure 2C–D, the Mg/Al LDH-5-OP-RU nanocomposite successfully transported GFP mRNA to the DCs. In the present study, positive GFP mRNA expression was observed in approximately 28% of the DCs, which was greater than that observed for LNP/GFP mRNA and naked GFP mRNA. Furthermore, less GFP mRNA expression in other cell types within the lung parenchyma and draining MLNs was observed after intranasal administration of Mg/Al LDH-5-OP-RU/GFP mRNA, suggesting specific targeting of DCs in the lung parenchyma and draining MLNs by Mg/Al LDH-5-OP-RU/GFP mRNA (Figure S4).

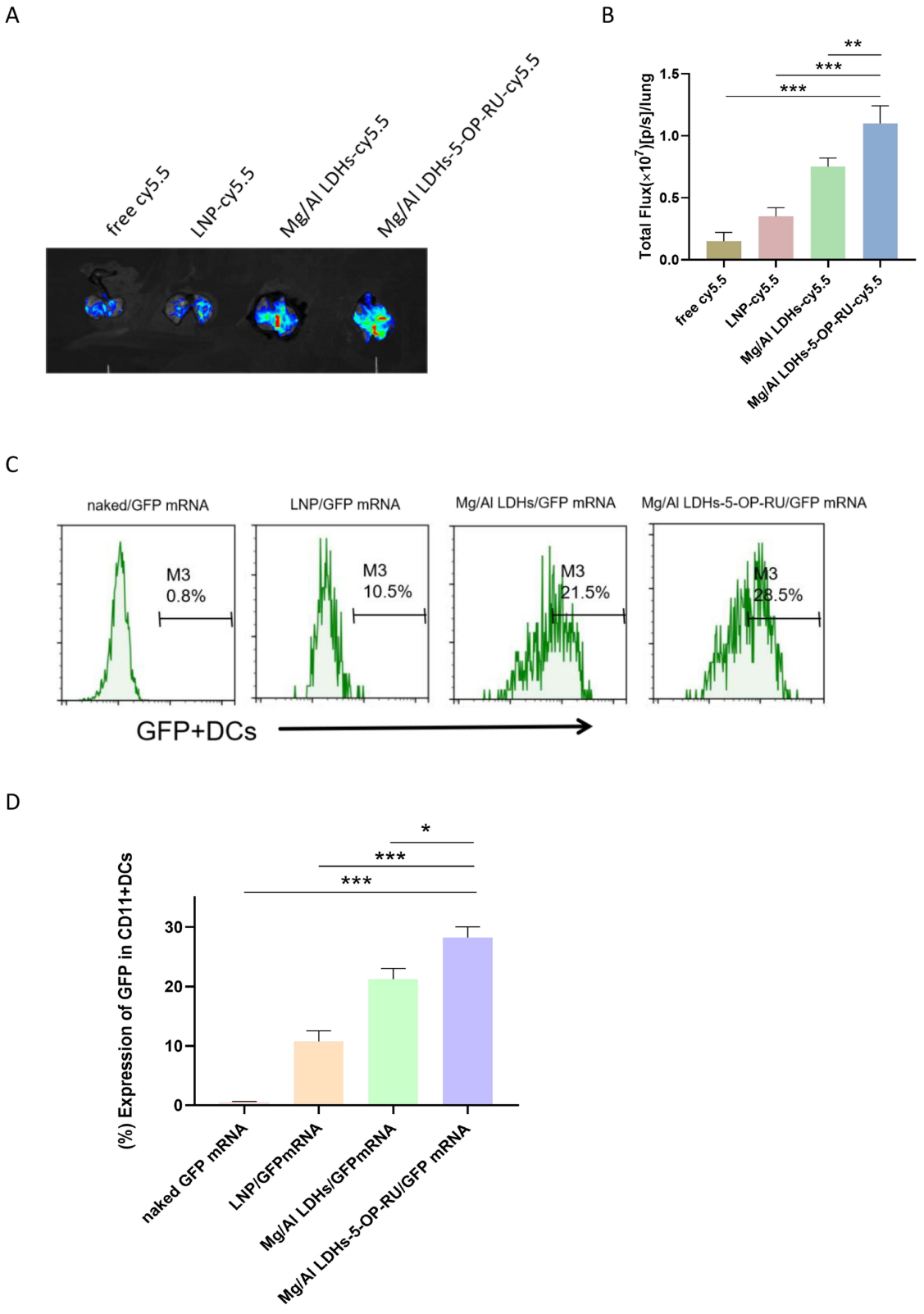

Figure 2 Intranasal administration of Mg/Al LDH-5-OP-RU promotes its accumulation in the lung parenchyma and draining MLNs, as well as promotes the transfection of DCs. (**A**) Representative images of bioluminescence within the lung after intranasal administration of Mg/Al LDH-5-OP-RU for 12 h. (**B**) Luminescence signal intensity of the lungs in (**A**). (**C** and **D**) Representative FACS histogram showing the frequencies and quantitative analysis of GFP-positive cells in DCs after intranasal administration of Mg/Al LDH-5-OP-RU/GFP mRNA nanovaccines for 48 h. The data are presented as the means ± SDs (n = 3). *P < 0.05, **P < 0.01, and ***P < 0.001.

Mg/Al LDH-5-OP-RU/mRNA may be more likely to target lymphoid tissues and be taken up by DC cells due to several reasons: 1) The size of the nanovaccine matches the follicular structure in the lymphatic system, making it easier for the vaccine to pass through the lymphatic system and be specifically delivered to lymphoid organs. 2) The zeta potential of Mg/Al LDHs-5-OP-RU/mRNA vaccine is +35mv, which is greater than the surface zeta potential of LNP/mRNA (+29 mv), making it more favorable for binding to and being taken up by cells; 3) previous studies have shown that only intramuscular (I.M.) immunization with the aluminum ions attracted APCs to the site of injection.[19,32,33] So intranasal immunization with the Mg/Al LDH-mRNA can attract APCs to the site of administration and is more easily captured by them; 4) moderate size of NPs was also contributed to endocytosis of APCs; 5) APCs have stronger phagocytosis ability than other cells.

Activation of MAIT Cells and DC Cells Induced by Mg/Al LDH-5-OP-RU Nanovaccine

Dendritic cells (DCs) are key antigen-presenting cells that are crucial for initiating the specific immune response induced by vaccines. Recent studies have shown that there is a strong positive correlation between lung-specific MAIT cells and T cell responses induced by vaccines, effectively linking adaptive and innate immunity pathways.[25,26] In the present study, 48 hours after the intranasal administration of Mg/Al LDH-5-OP-RU, Mg/Al LDH, free 5-OP-RU, or vehicle, the draining MLNs were harvested to assess the ability of Mg/Al LDH-5-OP-RU to activate MAIT cells and DC cells in the lung parenchyma and draining MLNs was evaluated by detecting the expression of surface costimulatory molecules on DCs and CD69 on MAIT cells. As shown in Figure 3A–D, Mg/Al LDH-5-OP-RU had the strongest stimulatory effect on DC cells and MAIT cells, as evidenced by the highest expression of CD80, CD86, MHC-II, and CD40 on DCs and the highest expression of CD69 on MAIT cells among the above immunization groups. Both Mg/Al LDH and free 5-OP-RU intranasal immunization also upregulated the expression of CD69 and costimulatory molecules on DCs, but the expression levels were lower than those in the Mg/Al LDH-5-OP-RU group.

Previous studies have demonstrated that MAIT cells activate DCs through the CD40-CD40L interaction,[25] and DCs activate MAIT cells through the secretion of IFN-α.[34] In line with these studies, the present study revealed that immunization with Mg/Al LDH-5-OP-RU increased CD40L levels on MAIT cells, and promoted the secretion of IFN-α in the BALF (Figure S5A–B). Blocking CD40 signaling with an α-CD40 antibody diminished costimulatory molecule expression on DCs but did not affect MAIT cell activation. Moreover, treatment with the IFN-α blocking antibody decreased CD69 expression on MAIT cells and costimulatory molecule expression on DCs (Figure 3E–F). Overall, these findings, coupled with studies in the lung, support the theory that intranasal administration of Mg/Al LDH-5-OP-RU concurrently stimulates the activation of both DCs and MAIT cells, after which both types of cells activate each other and can induce the activation and proliferation of MAIT cells and DCs to high levels via positive feedback.

Specific CD8+ T Cell Response Induced by Mg/Al LDH-5-OP-RU/mRNA Nanovaccine

As an mRNA vaccine carrier for targeting LNs, the present study demonstrated that Mg/Al LDH-5-OP-RU has high transfection efficiency and activation of DCs and MAIT cells. To further validate whether Mg/Al LDH-5-OP-RU, as an mRNA vaccine carrier, can effectively activate antigen-specific CD8+ T cells in vivo, we chose HPV E7, which can induce HPV-associated cancer, was used as the model antigen. The mRNA encoding the HPV E7 antigen was loaded into Mg/Al LDH-5-OP-RU to prepare the Mg/Al LDH-5-A-RU/E7 mRNA vaccine, which was then intranasally immunized into C57/B6 mice three times, with a one-week interval between each immunization. One week after the final immunization, the lung parenchyma and draining MLNs were removed from the mice, and a single-cell suspension was generated, followed by stimulation with the E7 antigen (Figure 4A). After 72 hours, E7 tetramer staining and intracellular cytokine staining were performed to test the activation and proliferation of E7-specific CD8+ T cells induced by the E7 antigen. As shown in Figure 4B–E, the percentage of IFN-γ+CD8+ and E7 tetramer+CD8+ T cells within total CD8+ T cells isolated from the Mg/Al LDH-5-OP-RU/E7 mRNA group reached approximately 2.4% and 3.3%, respectively, which was significantly greater than that of the LNP/E7 mRNA group (~1.7% and 2.5%, respectively) and the Mg/Al LDH/E7 mRNA group (~1.5% and 2.2%, respectively). Moreover, four weeks after the final vaccination, the IFN-γ+ cell levels were maintained above 2% in the Mg/Al LDH-5-OP-RU/E7 mRNA group, indicating the enduring immune memory prompted by the Mg/Al LDH-5-OP-RU/E7 mRNA vaccine and its potential for sustained protection

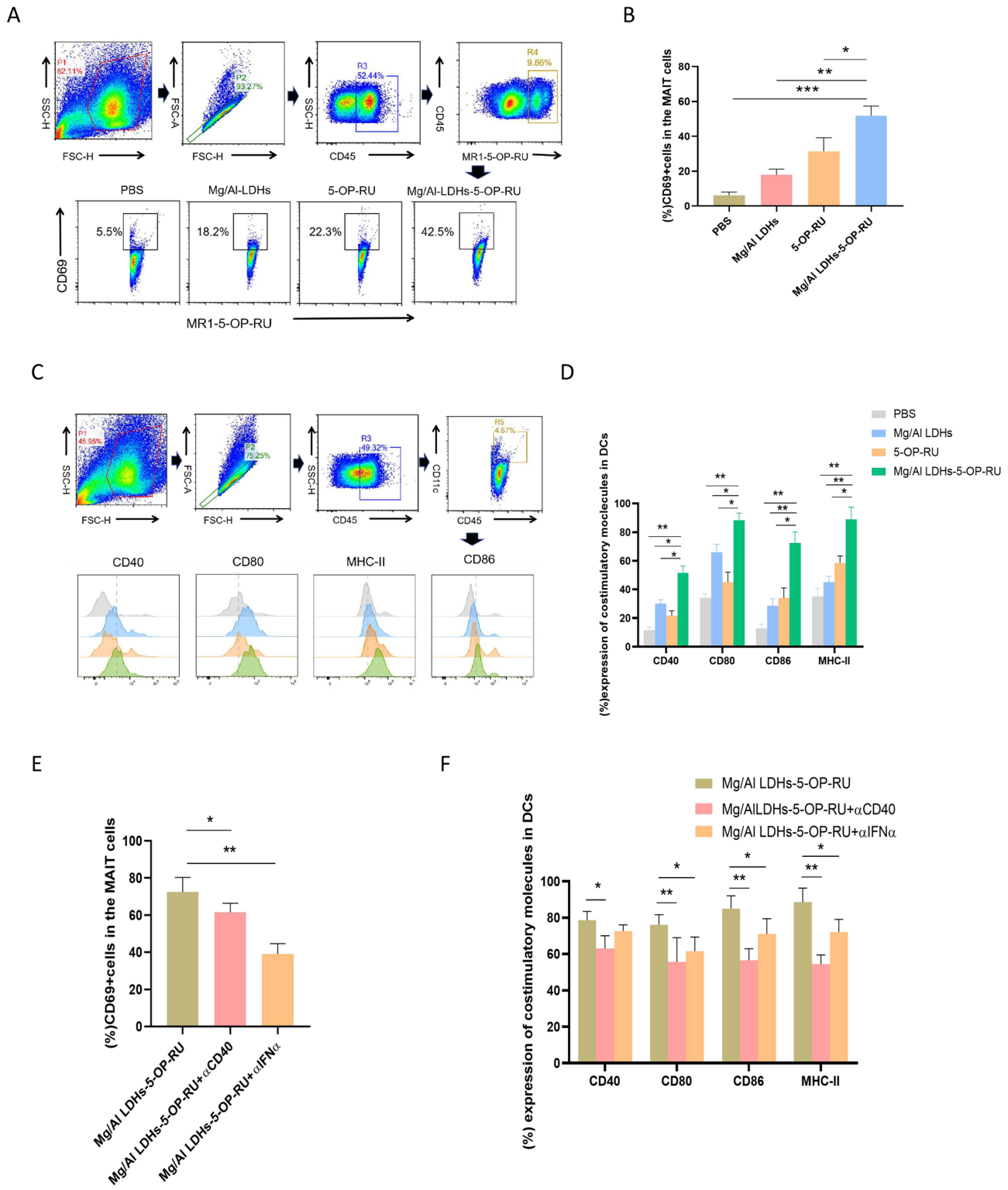

Figure 3 Intranasal administration of Mg/Al LDH-5-OP-RU enhances the activation and maturation of DCs and MAIT cells in the lung parenchyma and draining MLNs. (**A**) and (**B**) Quantitative flow cytometry analysis was used to measure the proliferation and activation of MAIT cells following exposure to Mg/Al LDH-5-OP-RU, free 5-OP-RU, and Mg/Al LDH. PBS served as a control. Representative FACS histogram and quantitative analysis of CD69 on MAIT cells. (**C** and **D**) Quantitative flow cytometry analysis was used to measure the maturation of dendritic cells (DCs) following exposure to Mg/Al LDH-5-OP-RU, free 5-OP-RU, or Mg/Al LDH. PBS treatment served as the control. Representative FACS histogram and quantitative analysis of costimulatory molecules (CD80, CD86, CD40, and MHCII) expression on DCs. (**E-F**) At 12 hours prior to and 1 h after i.n. vaccination, the mice were injected with 500 mg of αCD40L or αIFN-α intraperitoneally (i.p.), and the quantification of CD69 on MAIT cells (**E**) and costimulatory molecules on DCs (**F**) was conducted via flow cytometry. The data are presented as the means±SDs (n=5). Statistical significance was determined at *P < 0.05, **P < 0.01, and ***P < 0.001 vs cells treated with PBS.

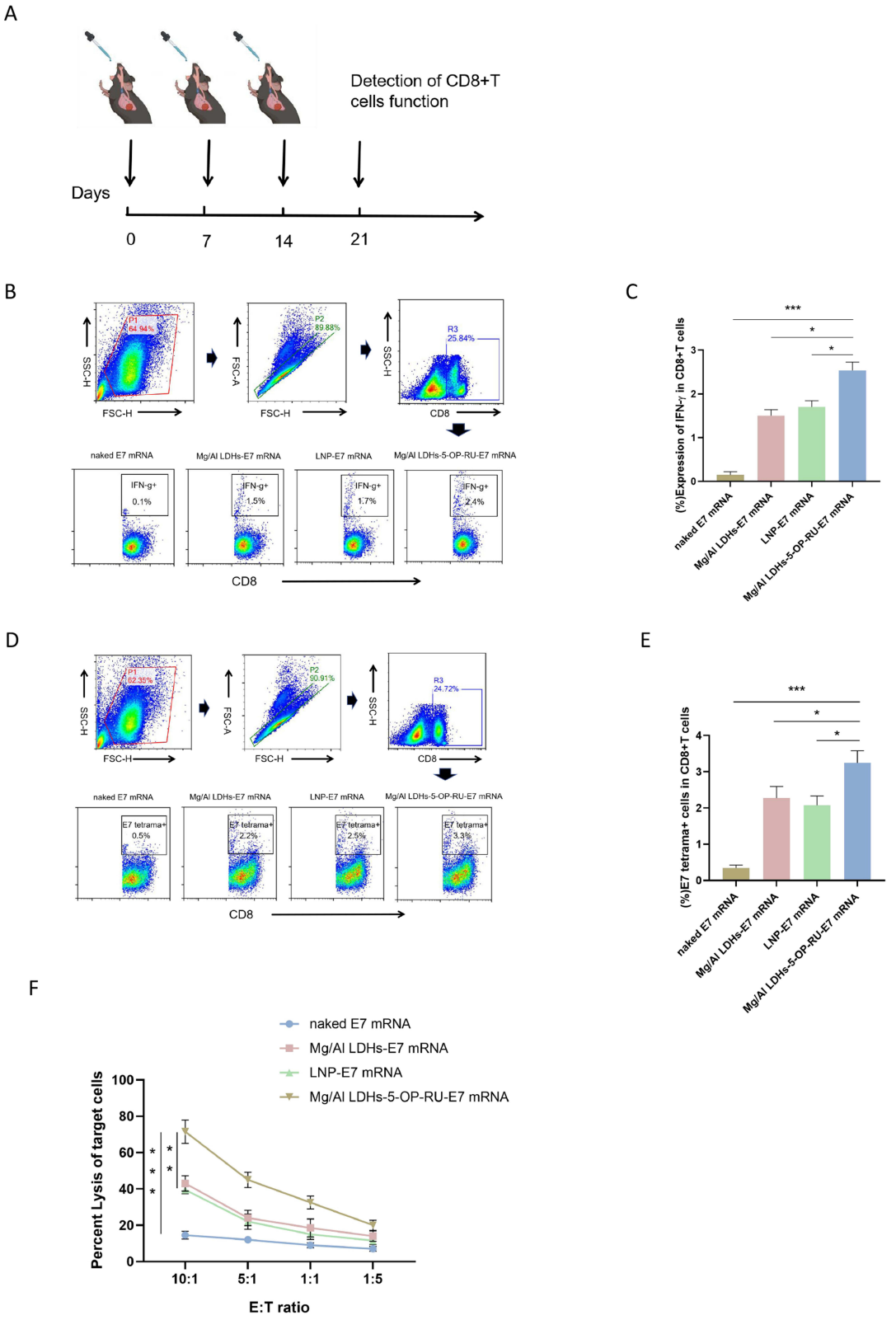

Figure 4 Intranasal administration of the Mg/Al LDH-5-OP-RU/E7 mRNA nanovaccine promotes E7-specific CD8+ T cell activation in the lung parenchyma and draining MLNs. (**A**) Schedule for detecting the activation and proliferation of E7-specific CD8+ T cells. (**B** and **E**) Scatter plots showing the frequencies and quantitative analysis of CD8+ IFN-γ+ T cells (**B, C**) and CD8+ E7-tetramer+ T cells (**D, E**) in the lung parenchyma and draining MLNs after intranasal administration of Mg/Al LDH-5-OP-RU/E7 mRNA, LNP/E7 mRNA, or Mg/Al LDH/E7 mRNA. Naked E7 mRNA treatment served as the control. (**F**) E7-specific CTL cytotoxicity after immunization with the vaccines. The results are presented as the means ± SDs (n=5). Statistical significance is presented as *P < 0.05, **P < 0.01, and ***P < 0.001.

https://doi.org/10.2147/IJN.S479741 DovePress

against tumor challenge (Figure S6A). Moreover, the CD8+ T cells in the lung parenchyma and draining MLNs after Mg/Al LDH-5-OP-RU/E7 vaccination expressed substantially higher levels of CD103 compared with cells in the other lymph nodes (Figure S6B), which suggested that the majority of lung antigen–specific CD8+ T cells were tissue-resident memory T cells.[35] Research has suggested that tissue-resident memory T cells make up the majority of E7-specific CD8+ T cells in the lung, highlighting their crucial role in providing protection against tumors arising from epithelial tissues.[2,36]

To further investigate the cytotoxicity of E7-specific CD8+ T cells induced by the Mg/Al LDH-5-OP-RU/E7 mRNA vaccine, CD8+ T cells isolated from the lung parenchyma and draining MLNs were cocultured with TC-1 cells expressing the E7 antigen after in vitro stimulation with the E7 protein. The CD8+ T cells from the mice immunized with the Mg/Al LDH-5-OP-RU/E7 mRNA vaccine had a stronger ability to kill tumor cells, with a killing efficiency of up to 70% at an effector-to-target ratio of 40:1, which was stronger than that of the Mg/Al LDH/E7 mRNA and LNP/E7 mRNA immunization groups (Figure 4F). However, CD8+ T cells in the spleen and inguinal lymph nodes did not significantly proliferate in E7-specific T cells after intranasal immunization (Figure S7A). These findings indicated that nasal immunity mainly induces local immune responses in the respiratory tract and lungs without causing systemic immune responses. Meanwhile, to verify the superiority of nasal immunity over other immune methods in inducing lung mucosal immunity, we subcutaneously immunized Mg/Al LDHs-5-OP-RU/E7 mRNA and observed the number of E7 specific CD8+T cells in lung lymphoid tissue. As shown in Figure S7B, no proliferation of E7 specific CD8+T cells was detected in the lung interstitium and draining lymph nodes after subcutaneous and intravenous immunization with Mg/Al LDHs-5-OP-RU/E7 mRNA, suggesting that subcutaneous immunization failed to effectively stimulate local mucosal immunity in the lung. Thus, Mg/Al LDH-5-OP-RU, as an mRNA vaccine carrier, effectively promotes the proliferation and activation of antigen-specific CD8+ T cells and initiates a strong mucosal cellular immune response in the lungs after intranasal administration.

Protective Effect of Mg/Al LDH-5-OP-RU/mRNA Nanovaccine

To determine whether the mucosal immune response induced by the Mg/Al LDH-5-OP-RU/E7 mRNA vaccine prevents lung metastasis, Mg/Al LDH-5-OP-RU/E7 mRNA, Mg/Al LDH/E7 mRNA, and LNP/E7 mRNA were intranasally immunized into the mice three times, with a one-week interval between each immunization. Naked E7 mRNA served as a control. Seven days after the intravenous injection of 5×10^5 TC-1-luc+ cells to mimic lung tumor metastasis, the growth of the tumors was quantified by measuring the luminescence intensity with an in vivo imaging system (IVIS) and averaging the region of interest (ROI) counts via Living Image 3.0 software (Figure 5A). As shown in Figure 5B–D, the mice treated with the Mg/Al LDH-5-OP-RU/E7 mRNA vaccine presented the slowest tumor progression. By Day 11, the fluorescence in the lungs of the mice treated with the Mg/Al LDH-5-OP-RU/E7 mRNA, Mg/Al LDH/E7 mRNA, and LNP/E7 mRNA vaccines was 24.7, 65.5, and 68% that of the control, respectively. Three weeks post-TC-1-luc challenge, the lungs were extracted, and the tumor nodules were counted. Compared with those in the control cohorts, the Mg/Al LDH-5-OP-RU/E7 mRNA, Mg/Al LDH/E7 mRNA, and 5-A-RU/E7 mRNA vaccines led to 5.7-, 1.7-, and 1.8-fold reductions in the number of tumor nodules, respectively. Next, rechallenge studies with TC-1-luc+ were performed to evaluate the longevity of immunity against lung metastasis from cancer cells. At 60 days after the last immunization, the mice were rechallenged with TC-1-luc+ cells, and tumor seeding in the lung was observed. As shown in Figure 5E–H, the fluorescence in the lungs of the mice treated with the Mg/Al LDH-5-OP-RU/E7 mRNA, Mg/Al LDH/E7 mRNA, and LNP/E7 mRNA vaccines was 40.8, 85.2, and 88% that of the control, respectively. Three weeks post-TC-1-luc+ challenge, the lungs were harvested, and the tumor nodules were counted. Compared with the naked E7 mRNA, the Mg/Al LDH-5-OP-RU/E7 mRNA led to a 3.2-fold decrease in the number of tumor nodules, indicating that the Mg/Al LDH-5-OP-RU/E7 mRNA vaccine induced a long-term protective effect against the lung metastasis of cancer cells. However, the Mg/Al LDH/E7 mRNA and 5-OP-RU/E7 mRNA vaccines did not reduce the number of tumor nodules in the lungs compared with the control and showed no long-term protective effects. Thus, the rechallenge experiment demonstrated the long-term protective effect of the Mg/Al LDH-5-OP-RU/E7 mRNA vaccine.

The findings from both the TC-1 challenge and rechallenge experiments revealed that the vaccine provides lasting protection against tumor spread in the lungs, a key factor in reducing the risk of tumor resurgence in post-surgery patients with circulating tumor cells in a clinical setting.

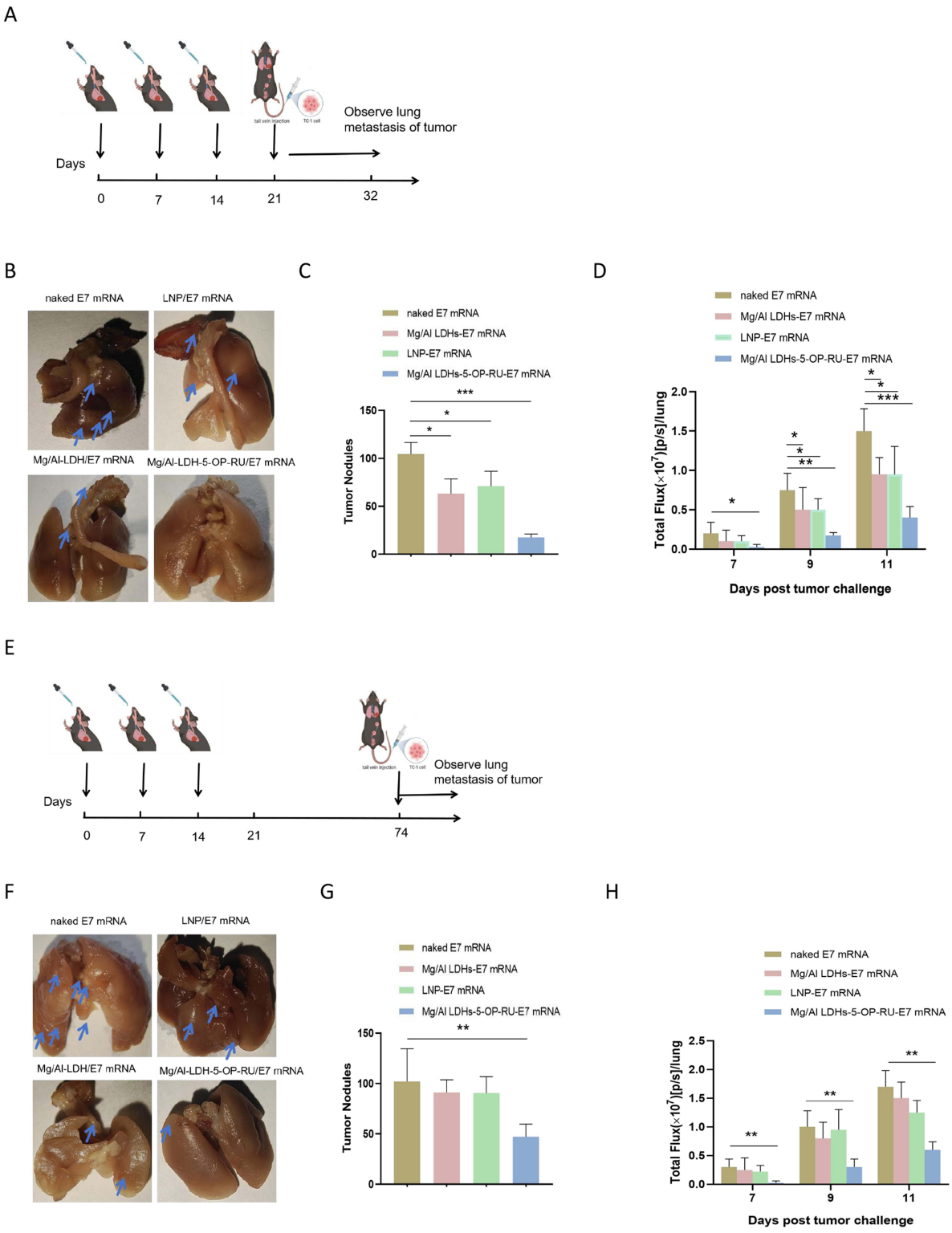

Figure 5 Intranasal administration of Mg/Al LDH-5-OP-RU/E7 mRNA nanovaccines increases protection against experimental lung metastasis of TC-1 cells. (**A**) Schedule for the prophylactic trial, showing triple intranasal immunization of C57BL/6 mice with the vaccines at one-week intervals followed by intravenous injection of 1×10^5 luc+TC-1 cells. (**B**) Representative lung images for each group. The white dots indicate TC-1 tumor nodules. (**C**) Quantitative assessment of TC-1 tumor nodules within the lungs displayed in the images **B**. The error bars represent the SDs. (**D**) Luminescence signal intensity of whole mice at 7, 9, and 11 days post-tumor challenge. (**E**) Schedule for the long-term protective effect experiment. C57BL/6 mice vaccinated with the indicated vaccines were i.v. injected with 1×10^5 luc+TC-1 cells 60 days after the last immunization. (**F**) Representative lung images for each group. The white dots indicate TC-1 tumor nodules. (**G**) Quantitative assessment of TC-1 tumor nodules within the lungs displayed in the images (**F**). (**H**) Luminescence signal intensity of whole mice at 7, 9, and 11 days post-tumor challenge. The results are reported as the means ± SDs (n=8). Statistical significance is presented as *P < 0.05, **P < 0.01, ***P < 0.001.

https://doi.org/10.2147/IJN.S479741 DovePress

Therapeutic Effect of Mg/Al LDH-5-OP-RU/mRNA Nanovaccine

Owing to the promising results of the mucosal mRNA cancer vaccine in preventing lung metastasis and given the potential significance for future clinical use in cancer treatment, the therapeutic potential of the Mg/Al LDH-5-OP-RU/E7 mRNA vaccine for existing lung metastatic tumors was evaluated.

The mice were intravenously injected with 5×10^5 TC-1 cells on Day 0. Subsequently, lung imaging was conducted every 2 to 4 days post-surgery. When the luminescence signal clearly appeared on Day 5, the metastatic tumor-bearing mice were treated with the Mg/Al LDH-5-OP-RU/E7 mRNA, Mg/Al LDH/E7 mRNA, and 5-OP-RU-E7 mRNA vaccines, as well as control vaccine, on Days 5, 10, and 15. The therapeutic efficiency was evaluated by measuring the luminescence, number of tumor nodes, and survival of the mice (Figure 6A). As shown in Figure 6B–D, the fluorescence in the lungs of the tumor-bearing mice treated with the Mg/Al LDH-5-OP-RU/E7 mRNA, Mg/Al LDH/E7 mRNA, and LNP/E7 mRNA vaccines was 45.2, 86.7, and 90% of the fluorescence of the naked E7 mRNA group, respectively. Two weeks after the TC-1-luc+ challenge, the lungs were harvested, and the tumor nodules in the lungs were manually counted. Compared with the naked E7 mRNA, the Mg/Al LDH-5-OP-RU/E7 mRNA led to a 2.8-fold decrease in the number of tumor nodules, whereas compared LDHs, the Mg/Al LDH/E7 mRNA and 5-OP-RU/E7 mRNA vaccines did not reduce the number of tumor nodules in the lungs. In terms of survival, the tumors developed quickly following the injection of tumor cells in the control animals, and by Day 30, only 20% of the control mice were alive. Moreover, treatment with the Mg/Al LDH/E7 mRNA and LNP/E7 mRNA vaccines inhibited metastatic tumor growth to a moderate degree, and 25% and 35% of the mice were alive at Day 40, respectively. In contrast, 72% of the mice in the Mg/Al LDH-5-OP-RU/E7 mRNA group survived until the final measurement on Day 40, with a tumor inhibition efficiency of 65% compared with that of the control group (Figure 6E). These findings suggested that Mg/Al LDH-5-OP-RU/E7 mRNA treatment significantly enhances therapeutic efficacy and increases survival rates in mice after intravenous tumor cell injection, potentially leading to the eradication of metastatic disease.

Analysis of Cytokines and Immune Cells in the Lung

The formation of microenvironments that facilitate cancer spread is known as the "premetastatic niche", which is essential for the growth and spread of metastatic cancer cells.[37,38] Premetastatic niche formation involves cytokines and immune cells. To gain insight into the impact of the Mg/Al LDH-5-OP-RU/E7 mRNA vaccine on cytokine expression and the composition of immune cells in established tumors, lung-infiltrating immune cells were evaluated after immunization via immunofluorescence staining. Compared with the control, immunofluorescence staining of lung sections revealed that the Mg/Al LDH-5-OP-RU/E7 mRNA vaccine diminished the accumulation of immunosuppressive cells, such as neutrophils and macrophages and increased aggregation of DCs, MAIT cells and CD8+T cells in metastatic tumors, suggesting an enhanced therapeutic effect. The Mg/Al LDH/E7 mRNA and LNP/E7 mRNA groups presented similar trends but to a lesser extent (Figure 7A). Neutrophils form NETs to attract tumor cells to the metastatic site.[39,40] Compared with those in the control group, the fractions of M1-like macrophages increased in the Mg/Al LDH-5-OP-RU/E7 mRNA, Mg/Al LDH-E7 mRNA, and LNP/E7 mRNA groups (Figure 7B–C). M2-like macrophages decreased in the Mg/Al LDH-5-OP-RU/E7 mRNA group, resulting in a favorable M1/M2 ratio, but this ratio was affected to a lesser extent in the other groups.

Cytokines in the lung tissues of immunized mice with metastatic tumors were detected via ELISA, including IL-10, IFNα, TGFβ, IFNγ, and IL-12, all of which are associated with the premetastatic niche and antitumor immune response. As shown in Figure 7D, compared with the other vaccines, the Mg/Al LDH-5-OP-RU/E7 mRNA vaccine induced sharp decreases in premetastatic niche-related cytokines and promoted immunostimulatory cytokine expression in the lung. Compared with those in the naked E7 mRNA group, the levels of IL-10 and TGFβ, which attract MDSCs, macrophages, and neutrophils to the premetastatic niche,[41] were decreased by 1.5- and 1.7-fold, respectively, in the Mg/Al LDH-5-OP-RU/E7 mRNA-vaccinated mice. Compared with those in control mice, the levels of the IFN-α and CXCL10 cytokines were significantly increased by 9.6-fold and 3.7-fold, respectively, in Mg/Al LDH-5-OP-RU/E7 mRNA-vaccinated mice. IFN-α stimulates MAIT cells, which can augment the CD8+ T cell immunity induced by vaccines through the integration of immunostimulatory signals.[24,42] The mechanism by which MAIT cell activation enhances vaccine-induced CD8+

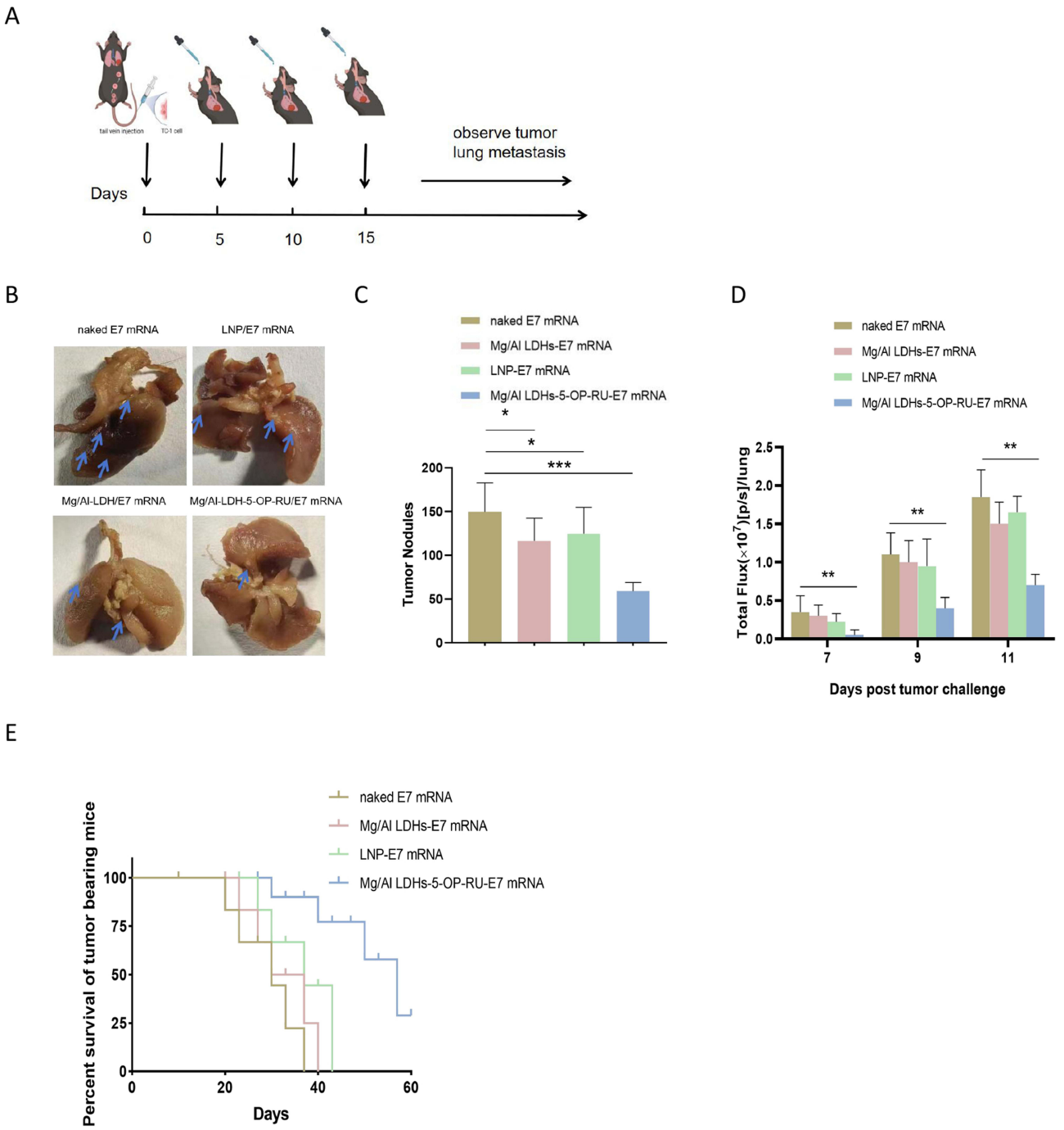

Figure 6 Therapeutic effects of intranasal administration of Mg/Al LDH-5-OP-RU/E7 mRNA nanovaccines against experimental lung metastasis of TC-1 cells. (**A**) Schedule for the therapeutic trial. C57BL/6 mice received an intravenous injection of 1×105 TC-1 cells on Day 0 and were then vaccinated intranasally with the vaccines indicated in the figure on Days 3, 6 and 10. (**B**) Representative lung images for each group were captured, with white dots indicating TC-1 tumor nodules. (**C**) Quantitative assessment of TC-1 tumor nodules within the lungs displayed in the images (**B**). The error bars represent the SDs. (**D**) Luminescence signal intensity of whole mice 7, 9, and 11 days after the tumor challenge and (**E**) the survival of the mice over time after vaccination (n = 8). Statistical significance is presented as *P < 0.05, **P < 0.01 and ***P < 0.001.

T cell immunity is still unknown. Some studies have shown that the CXCL10 chemokine may be an important candidate because it can enhance CD8+ T cell priming.[43] IFNγ and IL-12, which are immunostimulatory cytokines, showed a significant increase in the vaccinated mice. By the end of the third week, the level of IFNγ was 2.7 times higher in the vaccinated mice compared to the control group. While IL-12 could not be detected in the control mice using ELISA in the present study, it has been consistently detected in vaccinated mice at all times.[44] Both IFNγ and IL-12 are essential in

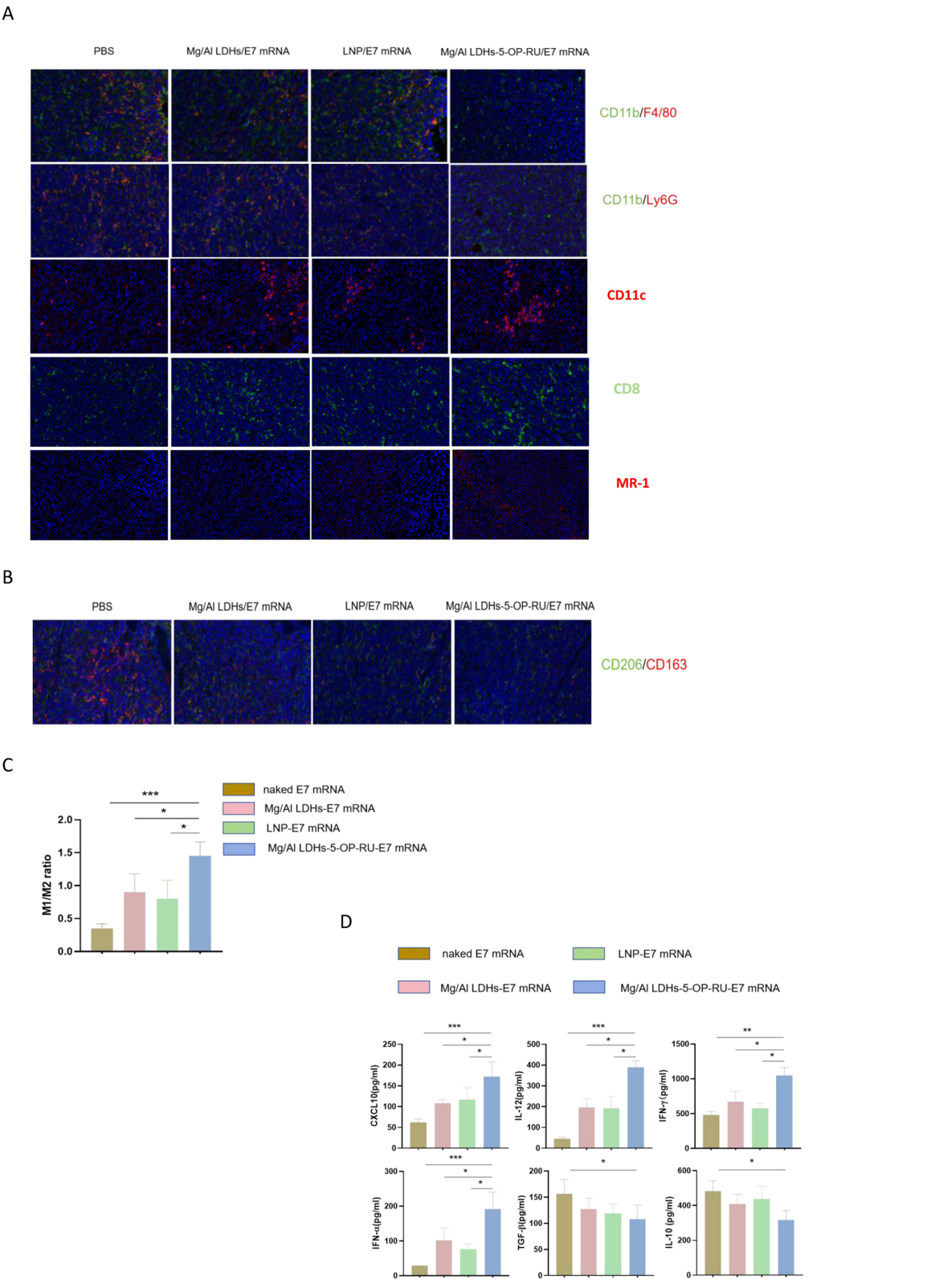

Figure 7 Analysis of cytokines and immune cells within the lungs or metastatic tumors of TC-1-i.v. injected mice after intranasal administration of Mg/Al LDH-5-OP-RU/E7 mRNA. (**A**) Immunofluorescence images of macrophages (F4/80+), neutrophils (ly6G+), DCs (CD11c+), MAIT (MR-1+) and CD8+T cells in tumors. (**B** and **C**) M1/M2 ratios in the lungs of vaccinated mice determined by immunofluorescence staining for iNOS (M1) or CD206 (M2). The data are presented as the means ± SDs (n=5). (**D**) Concentrations of IL-10, TGFβ, IFNα, IFNγ, IL-12, and CXCL10 in the BALF collected from immunized and control tumor-bearing C57BL/6 mice. The statistical analyses were performed with Student's *t* test, and the error bars represent SDs. *P < 0.05, **P < 0.01, and ***P < 0.001.

enhancing the immune response. IL-12 has a direct effect on enhancing the antitumoral functions of both natural killer cells and T cells, and it promotes the secretion of IFNγ.[45] IL-10 and TGFβ suppress the production of IL-12 in dendritic cells and M1 macrophages, and it inhibits antitumor immunity.[46]

Biosafety of Mg/Al LDHs-5-OP-RU/E7 mRNA Nanovaccine in vivo

Because the evaluation of vaccine safety is important for vaccine development, the present study evaluated the changes in the weights of the mice after vaccination. As shown in Figure S8A, no significant weight changes were observed in the immunized mice in each group after intranasal immunization, indicating a good biosafety of the vaccines. At the same time, the immunized mice were euthanized at the end of the experiment, and their peripheral blood and various organs were collected for blood biochemical analysis and HE staining. No abnormal histomorphological or pathological changes were observed in the organs of the immunized mice in each group (Figure S8B). Moreover, the serum levels of ALP, bilirubin, creatinine, and urea nitrogen were not significantly increased in the immunized mice in each group (Figure S8C–D), indicating that the vaccines did not cause damage to various tissues or organs. These results indicated that these vaccines have good biocompatibility and do not cause toxic side effects.

Conclusion

In summary, Mg/Al LDH-5-OP-RU is a superior carrier for mucosal mRNA cancer vaccines, as it can efficiently deliver mRNAs encoding tumor antigens into the lung parenchyma and draining MLNs to induce DC maturation and MAIT activation. The intranasal administration of the Mg/Al LDH-5-OP-RU/E7 mRNA vaccine elicits effective cellular immunity against cancer cells that have migrated in the lung and achieves robust protective and therapeutic effects, indicating broad potential for applications in immunotherapy for the lung metastasis of cancer cells. This system provides an excellent alternative delivery tool and an efficient delivery system for the development of mucosal mRNA-based cancer vaccines.

Data Sharing Statement

All the data needed to evaluate the findings in this study are included in the manuscript and/or the Supplementary Information.

Author Contributions

All authors made a significant contribution to the work reported, whether in the conception, study design, execution, data acquisition, data analysis, data interpretation, or in all these areas. All authors were involved in drafting, revising or critically reviewing the article, and they gave final approval of the version to be published. All authors agreed on the journal to which the article has been submitted, and they agreed to be accountable for all aspects of the work.

Funding

This work was financially supported by the National Natural Science Foundation of China (Grant No. 82073172), Natural Science Foundation of Shanghai (Grant No. 21ZR1466300; 21ZR1437500).

Disclosure

The authors declare that they have no conflicts of interest.

References

1. Jamil A, Kasi A. Lung Metastasis. In: *StatPearls*. FL, USA: StatPearls Publishing: Treasure Island; 2022.
2. Turner DL, Bickham KL, Thome JJ, et al. Lung niches for the generation and maintenance of tissue-resident memory T cells. *Mucosal Immunol*. 2014;7(3):501–510. doi:10.1038/mi.2013.67
3. Sandoval F, Terme M, Nizard M, et al. Mucosal imprinting of vaccine-induced CD8 + T cells is crucial to inhibit the growth of Mucosal tumors. *Sci Transl Med*. 2013;5(172):172ra20. doi:10.1126/scitranslmed.3004888
4. Kenoosh HA, Pallathadka H, Hjazi A, Al-Dhalimy AMB, Zearah SA. Recent advances in mRNA-based vaccine for cancer therapy; bench to bedside. *Cell Biochem Funct*. 2024;42(2):e3954. doi:10.1002/cbf.3954
5. Yao R, Xie C, Xia X. Recent progress in mRNA cancer vaccines. *Hum Vaccin Immunother*. 2024;20(1):2307187. doi:10.1080/21645515.2024.2307187

6. Pan S, Fan R, Han B, Tong A, Guo G. The potential of mRNA vaccines in cancer nanomedicine and immunotherapy. *Trends Immunol*. 2024;45(1):20–31. doi:10.1016/j.it.2023.11.003
7. Nembrini C, Stano A, Dane KY, et al. Nanoparticle conjugation of antigen enhances cytotoxic T-cell responses in pulmonary vaccination. *Proc Natl Acad Sci U S A*. 2011;108(44):E989–997. doi:10.1073/pnas.1104264108
8. Qiu F, Becker KW, Knight FC, et al. Poly(propylacrylic acid)- peptide nanoplexes as a platform for enhancing the immunogenicity of neoantigen cancer vaccines. *Biomaterials*. 2018;182:82–91. doi:10.1016/j.biomaterials.2018.07.052
9. Ballester M, Nembrini C, Dhar N, et al. Nanoparticle conjugation and pulmonary delivery enhance the protective efficacy of Ag85B and CpG against tuberculosis. *Vaccine*. 2011;29(40):6959–6966. doi:10.1016/j.vaccine.2011.07.039
10. Nizard M, Roussel H, Diniz MO, et al. Induction of resident memory T cells enhances the efficacy of cancer vaccine. *Nat Commun*. 2017;8(1):15221. doi:10.1038/ncomms15221
11. Webb JR, Milne K, Watson P, Deleeuw RJ, Nelson BH. Tumor-infiltrating lymphocytes expressing the tissue resident memory marker CD103 are associated with increased survival in high-grade serous ovarian cancer. *Clin Cancer Res*. 2014;20(2):434–444. doi:10.1158/1078-0432.CCR-13-1877
12. Donkor M, Choe J, Reid DM, et al. Nasal tumor vaccination protects against lung tumor development by induction of resident effector and memory anti-tumor immune responses. *Pharmaceutics*. 2023;15(2):445. doi:10.3390/pharmaceutics15020445
13. Mai Y, Guo J, Zhao Y, Ma S, Hou Y, Yang J. Intranasal delivery of cationic liposome-protamine complex mRNA vaccine elicits effective anti-tumor immunity. *Cell Immunol*. 2020;354:104143. doi:10.1016/j.cellimm.2020.104143
14. Yan L, Gonca S, Zhu G, Zhang W, Chen X. Layered double hydroxide nanostructures and nanocomposites for biomedical applications. *J Mater Chem B*. 2019;7(37):5583–5601. doi:10.1039/C9TB01312A
15. Li A, Qin L, Zhu D, et al. Signalling pathways involved in the activation of dendritic cells by layered double hydroxide nanoparticles. *Biomaterials*. 2010;31(4):748–756. doi:10.1016/j.biomaterials.2009.09.095
16. Chen WY, Zuo HL, Li B, et al. Clay nanoparticles elicit long-term immune responses by forming biodegradable depots for sustained antigen stimulation. *Small*. 2018;14(19):e1704465. doi:10.1002/smll.201704465
17. Li A, Qin L, Wang W, et al. The use of layered double hydroxides as DNA vaccine delivery vector for enhancement of anti-melanoma immune response. *Biomaterials*. 2011;32(2):469–477. doi:10.1016/j.biomaterials.2010.08.107
18. Yang L, Sun J, Liu Q, et al. Synergetic functional nanocomposites enhance immunotherapy in solid tumors by remodeling the immunoenvironment. *Adv Sci (Weinh)*. 2019;6(8):1802012. doi:10.1002/advs.201802012
19. Govea-Alonso DO, García-Soto MJ, Mendoza-Pérez ES, et al. Assessing the adjuvant effect of Layered Double Hydroxides (LDH) on BALB/c mice. *Materials*. 2023;16(15):5467. doi:10.3390/ma16155467
20. Wang J, Zhu R, Gao B, et al. The enhanced immune response of hepatitis B virus DNA vaccine using SiO2@LDH nanoparticles as an adjuvant. *Biomaterials*. 2014;35(1):466–478. doi:10.1016/j.biomaterials.2013.09.060
21. Li D, Xu M, Li G. Mg/Al-LDH as a nano-adjuvant for pertussis vaccine: a evaluation compared with aluminum hydroxide adjuvant. *Nanotechnology*. 2022;33(23):235102. doi:10.1088/1361-6528/ac56f3
22. Legoux F, Salou M, Lantz O. MAIT cell development and functions: the microbial connection. *Immunity*. 2020;53(4):710–723. doi:10.1016/j.immuni.2020.09.009
23. Amini A, Pang D, Hackstein C-P, Klenerman P. MAIT cells in barrier tissues: lessons from immediate neighbors. *Front Immunol*. 2020;11:58452. doi:10.3389/fimmu.2020.584521
24. Provine NM, Amini A, Garner LC, et al. MAIT cell activation augments adenovirus vector vaccine immunogenicity. *Science*. 2021;371(6528):521–526. doi:10.1126/science.aax8819
25. Soudais C, Samassa F, Sarkis M, et al. In vitro and in vivo analysis of the gram-negative bacteria-derived riboflavin precursor derivatives activating mouse MAIT cells. *J Immunol*. 2015;194(10):4641–4649. doi:10.4049/jimmunol.1403224
26. Hinks TSC, Marchi E, Jabeen M, et al. Activation and in vivo evolution of the MAIT cell transcriptome in mice and humans reveals tissue repair functionality. *Cell Rep*. 2019;28:3249–3262. doi:10.1016/j.celrep.2019.07.039
27. Pankhurst TE, Buick KH, Lange JL, et al. MAIT cells activate dendritic cells to promote TFH cell differentiation and induce humoral immunity. *Cell Rep*. 2023;42(4):112310. doi:10.1016/j.celrep.2023.112310
28. Wang H, Kjer-Nielsen L, Shi M, et al. IL-23 costimulates antigen-specific MAIT cell activation and enables vaccination against bacterial infection. *Sci Immunol*. 2019;4:eaaw0402.
29. Patel AK, Kaczmarek JC, Bose S, et al. Inhaled nanoformulated mRNA polyplexes for protein production in lung epithelium. *Adv Mater*. 2019;31(8):e1805116. doi:10.1002/adma.201805116
30. Pardi N, Hogan MJ, Weissman D. Recent advances in mRNA vaccine technology. *Curr Opin Immunol*. 2020;65:14–20. doi:10.1016/j.coi.2020.01.008
31. Pejoski D, Ballester M, Auderset F, et al. Site-specific DC surface signatures influence CD4+ T cell co-stimulation and lung-homing. *Front Immunol*. 2019;18:1650. doi:10.3389/fimmu.2019.01650
32. Zhang T, He P, Guo D, Chen K, Hu Z, Zou Y. Research progress of aluminum phosphate adjuvants and their action mechanisms. *Pharmaceutics*. 2023;15(6):1756. doi:10.3390/pharmaceutics15061756
33. Kooijman S, Vrieling H, Verhagen L, et al. Aluminum hydroxide and aluminum phosphate adjuvants elicit a different innate immune response. *J Pharm Sci*. 2022;111(4):982–990. doi:10.1016/j.xphs.2022.01.014
34. Turtle CJ, Delrow J, Joslyn RC, et al. Innate signals overcome acquired TCR signaling pathway regulation and govern the fate of human CD161(hi) CD8a+ semi-invariant T cells. *Blood*. 2011;118(10):2752–2762. doi:10.1182/blood-2011-02-334698
35. Schenkel JM, Fraser KA, Vezys V, Masopust D. Sensing and alarm function of resident memory CD8+ T cells. *Nat Immunol*. 2013;14(5):509–513. doi:10.1038/ni.2568
36. Schenkel JM, Fraser KA, Beura LK, Pauken KE, Vezys V, Masopust D. Resident memory CD8 T cells trigger protective innate and adaptive immune responses. *Science*. 2014;346(6205):98–101. doi:10.1126/science.1254536
37. Liu Y, Cao X. Characteristics and significance of the pre-metastatic niche. *Cancer Cell*. 2016;30(5):668–681. doi:10.1016/j.ccell.2016.09.011
38. Peinado H, Zhang H, Matei IR, et al. Pre-metastatic niches: organ-specific homes for metastases. *Nat Rev Cancer*. 2017;17(5):302–317. doi:10.1038/nrc.2017.6
39. Zuo H, Yang M, Ji Q, et al. Targeting neutrophil extracellular traps: a novel antitumor strategy. *J Immunol Res*. 2023;9:5599660.

40. Hu Y, Wang H, Liu Y. NETosis: sculpting tumor metastasis and immunotherapy. *Immunol Rev*. 2024;321(1):263–279. doi:10.1111/imr.13277
41. Goldmann O, Nwofor OV, Chen Q, Medina E. Mechanisms underlying immunosuppression by regulatory cells. *Front Immunol*. 2024;15:1328193. doi:10.3389/fimmu.2024.1328193
42. Pavlovic M, Gross C, Chili C, Secher T, Treiner E. MAIT cells display a specific response to type 1 IFN underlying the adjuvant effect of TLR7/8 ligands. *Front Immunol*. 2020;11:2097. doi:10.3389/fimmu.2020.02097
43. Russo E, Santoni A, Bernardini G. Tumor inhibition or tumor promotion? The duplicity of CXCR3 in cancer. *J Leukoc Biol*. 2020;108(2):673–685. doi:10.1002/JLB.5MR0320-205R
44. Parihar R, Dierksheide J, Hu Y, Carson WE. IL-12 enhances the natural killer cell cytokine response to Ab-coated tumor cells. *J Clin Invest*. 2002;110(7):983–992. doi:10.1172/JCI0215950
45. Castro F, Cardoso AP, Gonçalves RM, Serre K, Oliveira MJ. Interferon-gamma at the crossroads of tumor immune surveillance or evasion. *Front Immunol*. 2018;9(847). doi:10.3389/fimmu.2018.00847
46. Yaseen MM, Abuharfeil NM, Darmani H, Daoud A. Mechanisms of immune suppression by myeloid-derived suppressor cells: the role of interleukin-10 as a key immunoregulatory cytokine. *Open Biol*. 2020;10(9):200111. doi:10.1098/rsob.200111